UB-165: A Novel Nicotinic Agonist with Subtype Selectivity Implicates the $\alpha4\beta2$* Subtype in the Modulation of Dopamine Release from Rat Striatal Synaptosomes

Christopher G. V. Sharples,[1] Sergio Kaiser,[1] Lev Soliakov,[1] Michael J. Marks,[2] Allan C. Collins,[2] Mark Washburn,[3] Emma Wright,[4] James A. Spencer,[4] Timothy Gallagher,[4] Paul Whiteaker,[2] and Susan Wonnacott[1]

[1]Department of Biology and Biochemistry, University of Bath, Bath BA2 7AY, United Kingdom, [2]Institute for Behavioral Genetics, University of Colorado, Boulder, Colorado 80309, [3]SIBIA Neurosciences Inc., La Jolla, California 92037-4641, and [4]School of Chemistry, University of Bristol, Bristol BS8 1TS United Kingdom

Presynaptic nicotinic acetylcholine receptors (nAChRs) on striatal synaptosomes stimulate dopamine release. Partial inhibition by the $\alpha3\beta2$-selective α-conotoxin-MII indicates heterogeneity of presynaptic nAChRs on dopamine terminals. We have used this α-conotoxin and UB-165, a novel hybrid of epibatidine and anatoxin-a, to address the hypothesis that the α-conotoxin-MII-insensitive subtype is composed of $\alpha4$ and $\beta2$ subunits. UB-165 shows intermediate potency, compared with the parent molecules, at $\alpha4\beta2$* and $\alpha3$-containing binding sites, and resembles epibatidine in its high discrimination of these sites over $\alpha7$-type and muscle binding sites. (±)-Epibatidine, (±)-anatoxin-a, and (±)-UB-165 stimulated [^{3}H]-dopamine release from striatal synaptosomes with EC_{50} values of 2.4, 134, and 88 nM, and relative efficacies of 1:0.4:0.2, respectively. α-Conotoxin-MII inhibited release evoked by these agonists by 48, 56, and 88%, respectively, suggesting that (±)-UB-165 is a very poor agonist at the α-conotoxin-MII-insensitive nAChR subtype. In assays of $^{86}Rb^+$ efflux from thalamic synaptosomes, a model of an $\alpha4\beta2$* nAChR response, (±)-UB-165 was a very weak partial agonist; the low efficacy of (±)-UB-165 at $\alpha4\beta2$ nAChR was confirmed in *Xenopus* oocytes expressing various combinations of human nAChR subunits. In contrast, (±)-UB-165 and (±)-anatoxin-a were similarly efficacious and similarly sensitive to α-conotoxin-MII in increasing intracellular Ca^{2+} in SH-SY5Y cells, a functional assay for native $\alpha3$-containing nAChR. These data support the involvement of $\alpha4\beta2$* nAChR in the presynaptic modulation of striatal dopamine release and illustrate the utility of exploiting a novel partial agonist, together with a selective antagonist, to dissect the functional roles of nAChR subtypes in the brain.

Key words: neuronal nicotinic acetylcholine receptor; presynaptic nicotinic modulation; dopamine release; rat striatal synaptosomes; Xenopus *oocytes; SH-SY5Y cells; α-conotoxin*

Nicotinic acetylcholine receptors (nAChRs) are widely distributed in the vertebrate CNS. With a few recently reported exceptions (Alkondon et al., 1998; Frazier et al., 1998), most nAChRs in the brain do not appear to mediate synaptic transmission. Instead, their primary function may be modulatory (Role and Berg, 1996). One locus for modulation is the nerve terminal, where presynaptic nAChRs can promote transmitter release and hence influence resting tone or synaptic efficacy.

Presynaptic nAChRs facilitate the release of many neurotransmitters, in numerous brain regions, via various nAChR subtypes (Wonnacott, 1997). nAChR heterogeneity arises from the pentameric assembly of receptors from numerous α and β subunits ($\alpha2$–$\alpha7$, $\beta2$–$\beta4$) expressed in the mammalian brain (Role and Berg, 1996; Lukas et al., 1999). Defining the subunit composition of native nAChR is a major challenge; this quest is hampered by a lack of subtype-specific tools. A recent advance has been the identification of Conus toxins that target particular neuronal nAChR subtypes (McIntosh et al., 1999). α-Conotoxin-MII, with specificity for $\alpha3\beta2$-containing nAChRs (Cartier et al., 1996), partially inhibits the nicotinic stimulation of [^{3}H]-dopamine release from striatal preparations (Kulak et al., 1997; Kaiser et al., 1998), indicating heterogeneity of the nAChR mediating this response.

The nicotinic modulation of [^{3}H]-dopamine release from striatal preparations has been exploited as a model system for examining native nAChR responses (Soliakov and Wonnacott, 1996; Grady et al., 1997) and evaluating novel ligands (Holladay et al., 1997) and is pertinent to physiological and pathological processes (Dani and Heinemann, 1996; Decker and Arneric, 1998). Nicotinic agonists elicit dopamine release from rodent striatal synaptosomes and slices in a concentration-dependant manner, and this response is blocked by nicotinic antagonists, including mecamylamine and dihydroβerythroidine (Grady et al., 1992; El-Bizri and Clarke, 1994; Sacaan et al., 1995; Soliakov et al., 1995). Insensitivity to the $\alpha7$-selective antagonists α-bungarotoxin (αBgt) (Rapier et al., 1990; Grady et al., 1992) and α-conotoxin-ImI (Kulak et al., 1997) argues against the direct involvement of $\alpha7$ nAChR. The loss of [^{3}H]-nicotine binding sites from the striatum after 6-hydroxy-

Received Oct. 21, 1999; revised Jan. 27, 2000; accepted Feb. 7, 2000.

This work was supported by Biotechnology and Biological Sciences Research Council (BBSRC) Grants 7/MOLO4724 (T.C.) and 86/B11785 (S.W. and T.C.); BAT Co. Ltd. (S.W.); National Institute on Drug Abuse Grants DA-03194 and DA-00197 (A.C.C.); postgraduate studentships from BBSRC and Engineering and Physical Sciences Research Council to C.G.V.S. and J.A.S., respectively; and NATO Collaborative Research Grant CRG 971632 (S.W. and A.C.C.). We are grateful to Adrian Mogg for the assays on rat muscle.

Dr. Kaiser's present address: Department of Biology, University of California, San Diego, 9500 Gilman Drive, La Jolla, CA 92093-0357.

Correspondence should be addressed to Dr. S. Wonnacott, Department of Biology and Biochemistry, University of Bath, Bath, BA2 7AY, UK. E-mail: s.wonnacott@bath.ac.uk.

dopamine lesion of the nigrostriatal pathway is consistent with α4β2 nAChRs on striatal terminals (Clarke and Pert, 1985). Alternatively, sensitivity to neuronal bungarotoxin was interpreted in favor of α3-containing nAChRs (Grady et al., 1992). These disparate views are reconciled by the nAChR heterogeneity implicit in the partial inhibition by α-conotoxin-MII (Kulak et al., 1997; Kaiser et al., 1998). The selectivity of this toxin is consistent with an nAChR containing α3 and β2 subunits (Cartier et al., 1996; Kaiser et al., 1998); the α4β2* nAChR is a candidate for the α-conotoxin-MII-insensitive component of dopamine release evoked by nicotinic agonists.

Here we report studies with the novel nicotinic ligand UB-165 (Wright et al., 1997) (see Fig. 1) that support this interpretation. UB-165 is a hybrid of anatoxin-a and epibatidine, with potency at rat brain [^{3}H]-nicotine binding sites that is intermediate between the values of the parent molecules. We have extended the characterization of UB-165 and have exploited its limited agonism at α4β2 nAChRs to examine the putative contribution of this subtype to the nicotinic stimulation of striatal dopamine release.

MATERIALS AND METHODS

Materials

Cell culture. SH-SY5Y cells were from European Collection of Animal Cell Cultures (Porton Down, Salisbury, Wiltshire, UK) and were cultured as described by Murphy et al. (1991). M10 cells were provided by Dr. P. Whiting (Merck, Sharp and Dohme Research Center, Harlow, Essex, UK) and were cultured as described previously (Whiteaker et al., 1998). Cell culture media were provided by Life Technologies (Paisley, Renfrewshire, Scotland), and tissue culture plastic ware was obtained from Becton Dickinson UK Ltd. (Oxford, UK) and Sterilin (Stone, Staffordshire, UK).

Drugs and reagents. (−)-[^{3}H]-Nicotine (3.0 TBq/mmol in ethanol) and (±)-[^{3}H]-epibatidine (2.1 TBq/mmol in ethanol) were provided by Dupont NEN (Stevenage, Herts, UK) and stored at −20°C. ^{86}RbCl was obtained from Dupont NEN (Herts, UK or Boston, MA); it was stored at 20°C and used within 1 month. [7,8-^{3}H]-dopamine (specific activity, 1.78 TBq/mmol) was purchased from Amersham International (Buckinghamshire, UK) and stored at −20°C. Na^{125}I from Amersham International was used to iodinate αBgt to a specific activity of 26 TBq/mmol. (±)-Epibatidine was purchased from RBI (Natick, MA), and (±)-anatoxin-a was obtained from Tocris Cookson (Bristol, UK). Racemic UB-165 (Wright et al., 1997) and α-conotoxin-MII (Cartier et al., 1996; Kaiser et al., 1998) were synthesized as previously described. All other drugs and reagents were provided by Sigma (Poole, Dorset, UK).

Tissue preparations

Rat brain membranes. P2 membranes from whole rat brain (minus cerebellum) were prepared as previously described (Davies et al., 1999). Briefly, brains were homogenized (10% w/v) in ice-cold 0.32 M sucrose, pH 7.4, containing 1 mM EDTA, 0.1 mM PMSF, and 0.01% NaN_3, and centrifuged at 1000 × *g* for 10 min. The supernatant fraction (S1) was decanted and retained on ice. The pellet (P1) was resuspended in ice-cold 0.32 M sucrose (5 ml/g original weight) and recentrifuged at 1000 × *g* for 10 min. The supernatant was combined with S1 and centrifuged at 12,000 × *g* for 30 min. The pellet (P2) was resuspended (2.5 ml/g original weight) in phosphate buffer (50 mM potassium phosphate, pH 7.4, containing 1 mM EDTA, 0.1 mM PMSF, and 0.01% NaN_3), and washed twice by centrifugation at 12,000 × *g* for 30 min. The washed pellet was resuspended in phosphate buffer (2.5 ml/g original weight) and stored in 5 ml aliquots at −20°C.

Rat muscle extract preparation. A Triton X-100 extract of muscle from the hindlimbs of Wistar rats was prepared as previously described (Garcha et al., 1993).

SH-SY5Y cell membrane preparation. SH-SY5Y cells, grown to confluency in 175 cm^2 flasks, were washed briefly with warm PBS containing (in mM): (150 NaCl, 8 K_2HPO_4, 2 KH_2PO_4, pH 7.4, 37°C) and scraped into cold phosphate buffer. Cells were washed by centrifugation for 3 min at 500 × *g* and resuspended in 10 ml of ice-cold phosphate buffer. The suspension was homogenized for 10 sec using an Ultraturax and centrifuged for 30 min at 45,000 × *g*. The pellet was resuspended in phosphate buffer (0.5 ml per original flask).

Radioligand binding assays

(−)-[^{3}H]-nicotine competition binding assays: rat brain membranes. P2 membranes (250 μg protein) were incubated in a total volume of 250 μl in HEPES buffer (20 mM HEPES, pH 7.4, containing 118 mM NaCl, 4.8 mM KCl, 2.5 mM $CaCl_2$, 200 mM Tris, 0.1 mM PMSF, 0.01% (w/v) NaN_3) (Romm et al., 1990) with 10 nM (−)-[^{3}H]-nicotine and serial dilutions of test drugs. Nonspecific binding was determined in the presence of 100 μM (−)-nicotine. Samples were incubated for 30 min at room temperature followed by 1 hr at 4°C. The reaction was terminated by filtration through Whatman GFA/E filter paper (presoaked overnight in 0.3% polyethyleneimine in PBS), using a Brandel Cell Harvester. Filters were counted for radioactivity in 5 ml Optiphase "Safe" scintillant in a Packard Tricarb 1600 scintillation counter (counting efficiency 45%).

(±)-[^{3}H]-epibatidine competition binding assays. SH-SY5Y cells. SH-SY5Y membranes (30 μg protein) were incubated in a total volume of 2 ml in 50 mM phosphate buffer with 150 pM (±)-[^{3}H]-epibatidine and serial dilutions of test drugs. Nonspecific binding was determined in the presence of 100 μM (−)-nicotine. Samples were incubated for 2 hr at 37°C. They were filtered and counted for radioactivity as described above.

[^{125}I]-αBgt competition binding assays: rat brain membranes. P2 membranes (250 μg protein) were incubated in a total volume of 250 μl in 50 mM phosphate buffer with 1 nM [^{125}I]-αBgt and serial dilutions of test drugs (Davies et al., 1999). Nonspecific binding was determined in the presence of 10 μM αBgt. Samples were incubated for 3 hr at 37°C. Ice-cold PBS (0.5 ml) was then added, and the samples were centrifuged for 3 min at 10,000 × *g*. Pellets were washed by resuspension in 1.25 ml PBS and centrifugation as before. The resultant pellets were counted for radioactivity in a Packard Cobra II auto-gamma counter.

[^{125}I]-αBgt competition binding assays: rat muscle extract. Rat muscle extract (1.5 mg protein) was incubated in a total volume of 500 μl in 2.5 mM sodium phosphate buffer, pH 7.4, with 1 nM [^{125}I]-αBgt and serial dilutions of test drugs (Garcha et al., 1993). Nonspecific binding was determined in the presence of 10 μM αBgt. Samples were incubated for 2 hr at 37°C. Bound radioligand was separated by filtration through Whatman GF/C filters (presoaked in 0.3% polyethyleneimine in PBS overnight) using a Millipore vacuum manifold. Filters were washed three times with 3 ml cold PBS supplemented with 0.1% BSA and counted for radioactivity in a Packard Cobra II auto-gamma counter.

[^{3}H]-epibatidine binding to M10 cells. Total numbers of nicotinic binding sites in M10 cells were measured *in situ,* in cultures in 24-well plates incubated with 500 pM (±)-[^{3}H]-epibatidine for 2 hr, as previously described (Whiteaker et al., 1998). Competition binding assays were performed similarly, using 200 pM [^{3}H]-epibatidine and serial dilutions of test drugs.

Upregulation of [^{3}H]-epibatidine binding sites in M10 cells

M10 cells grown were grown in 24-well plates to ~70% confluency and were then incubated for 48 hr at 37°C with dexamethasone (to induce nAChR expression) in medium containing serial dilutions of test drugs (Whiteaker et al., 1998). Control cells, treated with dexamethasone in medium without the addition of nicotinic agents, were incubated in parallel. A rigorous washing procedure, in which medium was replaced three times at hourly intervals, was used to ensure removal of nicotinic drugs (Whiteaker et al., 1998) before assaying for [^{3}H]-epibatidine binding sites as outlined above.

Superfusion of rat striatal synaptosomes for [^{3}H]-dopamine release

P2 synaptosomes were prepared from rat striata, loaded with [^{3}H]-dopamine (0.1 μM, 0.132 MBq/ml) for 15 min at 37°C, and superfused in open chambers as previously described (Soliakov et al., 1995; Kaiser et al., 1998). Synaptosomes were superfused with Krebs bicarbonate buffer containing (in mM): 118 NaCl, 2.4 KCl, 2.4 $CaCl_2$, 1.2 $MgSO_4$, 1.2 K_2HPO_4, 25 $NaHCO_3$ and 10 glucose, titrated to pH 7.4 with 95% O_2/5% CO_2, supplemented with 1 mM ascorbic acid, 8 μM pargyline, and 0.5 μM nomifensine to prevent dopamine degradation and reuptake. Agonists were applied for 40 sec. In antagonist studies, α-conotoxin-MII (112 nM) or mecamylamine (10 μM) was added to the superfusion buffer 10 min before the application of agonist and maintained throughout the remainder of the experiment. Experiments always included chambers stimu-

lated in parallel with 1 μM (±)-anatoxin-a, as a standard for normalization of data between experiments.

$^{86}Rb^+$ efflux from thalamic synaptosomes

$^{86}Rb^+$ efflux experiments were performed essentially as described by Marks et al. (1996). P2 synaptosomes were prepared from mouse or rat thalamus by homogenization in 0.32 M sucrose in 5 mM HEPES, pH 7.5, and differential centrifugation (Soliakov et al., 1995). Synaptosomes were loaded with $^{86}Rb^+$ (sufficient to give ~70 MBq per chamber) by incubation for 30 min at 22°C in uptake buffer containing (in mM): 140 NaCl, 1.5 KCl, 2.0 $CaCl_2$, 1.0 $MgS0_4$, 25 HEPES, 20 glucose, pH 7.5. Uptake was terminated, and unincorporated $^{86}Rb^+$ was removed by transferring aliquots (mouse, 25 μl; rat, 35 μl) to glass fiber filters for gentle filtration and washing. One thalamus provided sufficient material for up to 8 (mouse) or 12 (rat) filters. Each filter was placed in an open chamber of a superfusion apparatus (Marks et al., 1993; Soliakov et al., 1995). Samples were perfused at a rate of 2.5 ml/min with physiological buffer [135 mM NaCl,, 1.5 mM KCl, 2.0 mM $CaCl_2$, 1.0 mM $MgS0_4$, 20 mM glucose, 25 mM HEPES, pH 7.5, containing 0.1% (w/v) BSA; 5 mM CsCl and 50 nM tetrodotoxin]. After perfusion for 6 min, 12 samples were collected at 30 sec intervals. Agonist stimulation (60 sec) was given 90 sec after the start of sample collection. Where used, antagonists were present in the perfusion buffer throughout the experiment.

Xenopus *oocyte preparation and recording*

Stage V–VI oocytes were isolated from anesthetized *Xenopus laevis* frogs and enzymatically defolliculated by gentle shaking with collagenase [Worthington (Freehold, NJ), Type II, 1.7 mg/ml for 90 min; then Sigma (St. Louis, MO), Type II, 1.7 mg/ml for 30 min] in a Ca^{2+}-free Barth's solution. After defolliculation, oocytes were incubated at 16–19°C in a solution containing (in mM): 77.5 NaCl, 2 KCl, 1.8 $CaCl_2$, 1 $MgCl_2$, 5 HEPES, pH 7.5, adjusted with NaOH, and supplemented with 100 U/ml penicillin, 100 μg/ml streptomycin, 50 mg/ml gentimycin, and 5% heat-inactivated horse serum. Oocytes were injected the next day with 10–50 ng of mRNA encoding αx and βx nAChR subunits in an injection volume of 50 nl. The human nAChR subunits α2, α3, α4–2, β2, β4, and α7 were cloned from cDNA libraries prepared from human brain and the human IMR32 neuroblastoma cell line (Elliott *et al.,* 1996). For two-way combinations, RNA was injected at a ratio of 1:1 (25 ng of each subunit per egg). RNA for α7 was injected at a concentration of 25 ng per egg.

Oocytes were examined for functional expression 2–5 d after mRNA injection using two-electrode voltage-clamp techniques described previously (Chavez-Noriega et al., 1997). Agonist-induced currents were elicited at a holding potential of −60 mV. The recording solution contained (in mM): 115 NaCl, 2.5 KCl, 1.8 $CaCl_2$, 10 HEPES, 0.001 atropine, pH 7.3. Recording electrodes (0.5–2.5 MΩ resistance) were filled with 3 M KCl. Perfusion solutions were gravity fed into the recording chamber (capacity, 100 μl) at a rate of ~6–10 ml/min. All recordings were performed at room temperature (19–23° C). Signals were amplified, digitized (100–500 Hz), and filtered (at 40–200 Hz).

Calcium fluorimetry

SH-SY5Y cells, grown to confluency in 175 cm^2 flasks, were removed by incubation in Ca^{2+}-free PBS for 3 min at 37°C. The cell suspension was centrifuged for 3 min at 500 × *g*, and the pellet was resuspended in 3–4 ml Ca^{2+}-free HEPES buffer containing (in mM): 145 NaCl, 5 KCl, 1 $MgCl_2$, 0.5 Na_2HPO_4, 5.5 glucose, and 10 HEPES, pH 7.4, containing 5 μM fura-2 AM. The suspension was incubated in darkness at room temperature for 45 min, and excess fura-2 AM was removed by centrifugation for 3 min at 500 × *g* followed by three wash/centrifugation steps. Cell density was adjusted to 1–2 × 10^6 cells/ml, and a 2 ml aliquot of cell suspension was placed in a cuvette in a PTI dual-excitation spectrophotofluorimeter (Photon Technology International, South Brunswick, NJ). To the cell suspension, 2 mM $CaCl_2$ was added before applying a nicotinic agonist ((±)-UB-165 or (±)-anatoxin-a). Where used, the antagonist α-conotoxin-MII (112 nM) or mecamylamine (10 μM) was added to the cuvette 5 min before the addition of agonist. Excitation at 340 and 380 nm and emission at 510 nm were monitored. Calibration was performed in each experiment by adding sequentially 0.5% (v/v) Triton X-100 and 10 mM EDTA to derive maximum and minimum fluorescence ratios, respectively. Results were normalized within each experiment with respect to a maximally stimulating concentration of agonist.

Data analysis

Competition binding. IC_{50} values were calculated by fitting data points to the Hill equation, using the nonlinear least squares curve fitting facility of Sigma Plot V2.0 for windows. K_i values were derived from IC_{50} values according to the method of Cheng and Prusoff (1973), assuming K_d values of 10 and 1 nM for [^{3}H]-nicotine and [^{125}I]-αBgt binding to rat brain membranes and 0.12 nM for [^{125}I]αBgt binding to rat muscle, respectively.

$^{86}Rb^+$ efflux. Agonist-induced $^{86}Rb^+$ efflux was calculated as the fractional release above baseline on agonist stimulation (Marks et al., 1996). Basal efflux was defined as cpm collected in the fractions immediately before and after stimulation, and the basal rate of $^{86}Rb^+$ efflux was determined as an exponentially decaying curve fitted to these data points. Agonist-stimulated efflux was calculated as the cpm above the calculated baseline during the period of agonist application. To correct for interexperimental variation in synaptosomal $^{86}Rb^+$ uptake, agonist-stimulated efflux was divided by the calculated baseline efflux. Values for $^{86}Rb^+$ efflux from mouse thalamic synaptosomes are more than double those from corresponding rat preparations (see Fig. 5), reflecting the higher density of [^{3}H]-nicotine binding sites in mouse thalamus. Curve fitting of $^{86}Rb^+$ efflux data from mouse thalamic synaptosomes was performed using the nonlinear least squares curve fitting facility of Sigma Plot V5.0 for DOS.

Upregulation. Upregulation profiles were fit to a logistic equation (Whiteaker et al., 1998) using the nonlinear least squares curve fitting facility of Sigma Plot V2.0 for Windows, to give the EC_{50} for the upward phase of the dose–response curve and U_{max}, the maximum upregulation produced by the drug tested.

Dopamine release. Evoked [^{3}H]-dopamine release was calculated as the area under the peak, after subtraction of the baseline, as described previously (Kaiser et al., 1998). Data points for agonist dose–response relationships (after subtraction of nonspecific release determined in the presence of mecamylamine) were fitted to the Hill equation $y = (a - d)/[1 + (k/x)^n] + d$, where a is the asymptotic maximum, d is the asymptotic minimum, k is the agonist concentration at the inflection point (EC_{50}), x is the ligand concentration, and n is the slope parameter (Hill number).

Data for inhibition by antagonist are represented as percentages of the corresponding controls, assayed in parallel in the absence of antagonist. One-way ANOVA–*post hoc* Bonferroni test was used to determine the significance of differences from control.

Two-electrode voltage-clamp recordings. Full dose–response curves were obtained from individual oocytes and normalized relative to the response to an EC_{50} concentration of ACh recorded in the same oocyte. Sigmoidal concentration–response curves were fit to the Hill equation using Origin 4.0 (Microcal Software).

Calcium fluorimetry. The intracellular Ca^{2+} concentration ($[Ca^{2+}]_i$) was calculated from the fluorescence ratio of fura-2 (A_{340}/A_{380}, given as R below) according to the Grynkiewicz equation (Grynkiewicz et al., 1985) $[Ca^{2+}]_i = K_d * [(R - R_{min})/(R_{max} - R)]*(S_{f2}/S_{b2})$, where K_d is the dissociation constant for Ca^{2+} binding to fura-2, R_{min} is the fluorescence ratio under nominally "zero" free Ca^{2+} conditions, R_{max} is the fluorescence ratio under saturating Ca^{2+} conditions, and S_{f2}/S_{b2} is the ratio of fluorescence values of Ca^{2+}-free and Ca^{2+}-saturated fura-2, measured at the wavelength used to monitor Ca^{2+}-free fura-2.

For dose–response curves, agonist responses were calculated as the percentage of the change in intracellular Ca^{2+} produced by a maximally stimulating concentration of the same agonist, assayed in parallel. EC_{50} values were calculated by fitting data points to the Hill equation, using the nonlinear least squares curve fitting facility of Sigma Plot V2.0 for Windows.

RESULTS

Competition binding assays

(±)-UB-165 was compared with (±)-anatoxin-a and (±)-epibatidine (see Fig. 1 for structures) for its ability to displace the binding of a number of nicotinic radioligands (Fig. 2, Table 1). Radioligand binding assays, at least those using radiolabeled agonists, reflect the desensitized state of the nAChRs. Most high-affinity [^{3}H]-nicotine binding sites in rat brain are considered to represent the $\alpha4\beta2$ subtype (Zoli et al., 1998). (±)-Anatoxin-a and (±)-epibatidine inhibited [^{3}H]-nicotine binding

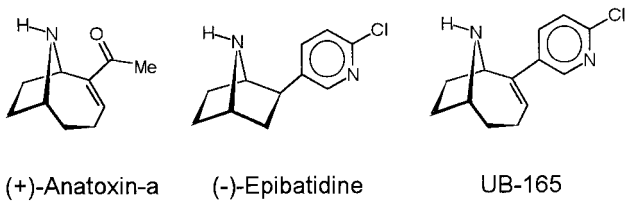

Figure 1. Molecular structures of (−)-epibatidine and (+)-anatoxin-a and the enantiomer of UB-165 that corresponds to (+)-anatoxin-a.

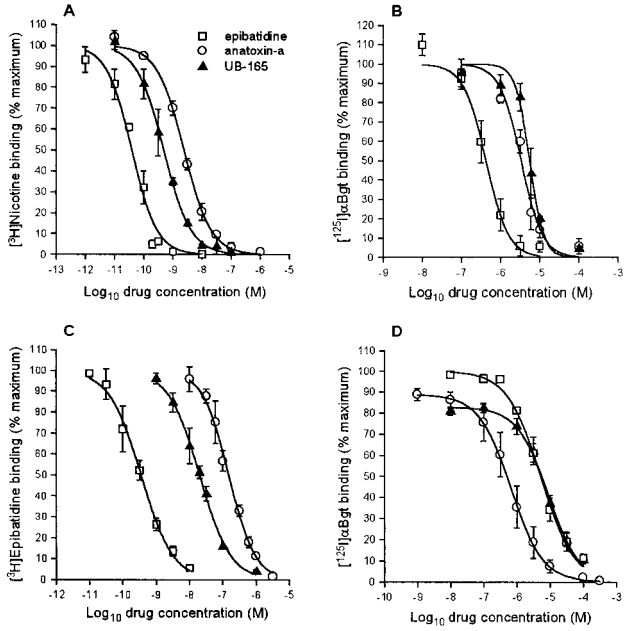

Figure 2. Competition binding assays for [^{3}H]-nicotine binding sites (*A*) and [^{125}I]-αBgt binding sites (*B*) in rat brain membranes, [^{3}H]-epibatidine binding sites (*C*) *in human SH-SY5Y cell membranes, and [^{125}I]-αBgt binding sites (D) in rat muscle extract. Preparations were incubated with radioligand and increasing concentrations of (±)-UB-165 (▲), (±)-anatoxin-a (○), or (±)-epibatidine (□) as described in Materials and Methods. Each point is the mean of at least three separate determinations ± SEM. Data points were fitted to the Hill equation.*

with K_i values of 1.25 ± 0.20 and 0.02 ± 0.005 nM, respectively. (±)-UB-165 displayed an intermediate potency, with a K_i value of 0.27 ± 0.05 nM (Fig. 2*A*, Table 1). Comparable K_i values were derived for inhibition of [^{3}H]-epibatidine binding to chicken α4β2 nAChRs in M10 cells (Table 1). (±)-Anatoxin-a and (±)-epibatidine competed with [^{125}I]-αBgt for binding to putative α7-type nAChRs in rat brain membranes, with K_i values of 1840 ± 260 and 233 ± 69 nM, respectively. (±)-UB-165 exhibited slightly lower potency than (±)-anatoxin-a, having a K_i value of 2790 ± 370 nM (Fig. 2*B*).

[^{3}H]-Epibatidine labels α3-containing nAChRs in human neuroblastoma SH-SY5Y cells (Wang et al., 1996). The concentration of [^{3}H]-epibatidine used (150 pM) was chosen to preferentially label α3β2-containing nAChRs [including α3β2 and α3β2α5 combinations (Wang et al., 1996)], but K_i values have not been derived because of the inherent nAChR heterogeneity. (±)-UB-165 displaced [^{3}H]-epibatidine from SH-SY5Y cell membranes with an IC_{50} value of 20 ± 0.7 nM, intermediate between that of (±)-anatoxin-a (IC_{50} = 155 ± 25 nM) and (±)-epibatidine (IC_{50} = 0.34 ± 0.06 nM) (Fig. 2*C*). (±)-UB-165 was also examined for its ability to displace [^{125}I]-αBgt from rat muscle extract (Fig. 2*D*). Its K_i value of 990 ± 240 nM was similar to that of (±)-epibatidine (K_i = 610 ± 160 nM), whereas (±)-anatoxin-a was the most potent competing ligand, with a K_i value of 85 ± 41 nM.

Thus the rank order of potencies at the rat and chicken α4β2 and human α3-containing nAChR subtypes is (±)-epibatidine > (±)-UB-165 > (±)-anatoxin-a. In contrast, (±)-UB-165 was the least potent at α7-type nAChRs and muscle nAChRs: rank orders of potencies are (±)-epibatidine > (±)-anatoxin-a ≥ (±)-UB-165 and (±)-anatoxin-a > (±)-epibatidine ≥ (±)-UB-165, respectively. The ability of each of these ligands to discriminate between nAChR subtypes was expressed as an affinity ratio, relative to the value at the rat brain [^{3}H]-nicotine binding site, which was defined as 1 (Table 1). From comparison of these affinity ratios, (±)-UB-165 resembles (±)-epibatidine in its marked preference for α4β2* nAChRs compared with α7-type and muscle nAChRs.

Upregulation of α4β2 nAChRs

(±)-Epibatidine and (±)-anatoxin-a differ in their abilities to upregulate α4β2 nAChRs in the M10 cell line: (±)-epibatidine is a partial upregulator whereas (±)-anatoxin-a is fully efficacious (Whiteaker et al., 1998). (±)-UB-165 was compared with (±)-anatoxin-a and (±)-epibatidine in this assay, to determine which of the parent compounds it most resembles with respect to upregulation (Fig. 3). Dose–response profiles for upregulation produced by (±)-UB-165 and (±)-anatoxin show that they are similarly efficacious, with maximum upregulation of 237 ± 47 and 221 ± 27% above control levels, respectively. (±)-UB-165 was a more potent upregulator than (±)-anatoxin-a, with EC_{50} values of 25.3 ± 17.7 and 985 ± 515 nM, respectively. In contrast, (±)-epibatidine achieved a maximum upregulation of only 76 ± 6% above control, although it was the most potent of the three ligands, with an EC_{50} value of 1.2 ± 0.2 nM. The ability of (±)-UB-165 to upregulate nicotinic binding sites is consistent with it behaving as an agonist at α4β2 nAChRs, because all agonists that we have examined have produced some degree of upregulation in this system, whereas antagonists produce little if any upregulation (Whiteaker et al., 1998).

Presynaptic nicotinic stimulation of [^{3}H]-dopamine release from rat striatal synaptosomes

(±)-UB-165 was compared with (±)-anatoxin-a, (±)-epibatidine, and (−)-nicotine for their abilities to promote [^{3}H]-dopamine release from rat striatal synaptosomes (Fig. 4*A*). Of these four compounds, (±)-epibatidine was the most efficacious and most potent (EC_{50} value = 2.42 ± 0.44 nM), whereas (−)-nicotine (EC_{50} value = 1.59 ± 0.38 μM) was the least potent but had higher efficacy than (±)-anatoxin-a. Although (±)-UB-165 was slightly more potent than (±)-anatoxin-a (EC_{50} values = 88 ± 18 and 134 ± 26 nM, respectively), it was much less efficacious than the other agonists, achieving a maximum of specific, nAChR-mediated [^{3}H]-dopamine release that was only 42% of that of (±)-anatoxin-a and 21% of that of (±)-epibatidine.

nAChRs mediating the presynaptic nicotinic stimulation of [^{3}H]-dopamine release from striatal terminals appear to be heterogeneous, based on the partial inhibition by the α3β2-selective toxin α-conotoxin-MII (Kulak et al., 1997; Kaiser et al., 1998). A maximally effective concentration of this toxin (112 nM) was compared with mecamylamine (10 μM) for their abilities to inhibit

Table 1. Affinities for radioligand binding sites corresponding to various nAChR subtypes

	Preparation:	Rat brain membranes		M10 cells		Rat brain membranes		Rat muscle extract		Human SH-SY5Y cells
	Radioligand:	[^{3}H]-nicotine binding		[^{3}H]-epibatidine binding		[^{125}I]-αBgt binding		[^{125}I]-αBgt binding		[^{3}H]-epibatidine binding
	nAChR subtype:	$\alpha4\beta2^{*a}$		chicken $\alpha4\beta2$		$\alpha7^{*a}$		$\alpha1\beta1\delta\epsilon$		$\alpha3^{*a}$
Agonists		K_i (nM)	Potency relative to rat $\alpha4\beta2$	K_i (nM)	Potency relative to rat $\alpha4\beta2$	K_i (nM)	Potency relative to rat $\alpha4\beta2$	K_i (nM)	Potency relative to rat $\alpha4\beta2$	IC_{50} (nM)
(±)-Epibatidine		0.021 ± 0.005	1	0.018 ± 0.003	1.2	233 ± 69	0.00009	610 ± 160	0.00044	0.340 ± 0.06
(±)-Anatoxin-a		1.25 ± 0.2	1	4.2 ± 0.8	0.29	1840 ± 260	0.00068	85 ± 41	0.015	155 ± 25
(±)-UB-165		0.27 ± 0.05	1	0.44 ± 0.13	0.62	2790 ± 374	0.00010	990 ± 240	0.00027	20 ± 0.7

[a] *, denotes possible presence of additional undefined subunits, according to the recommendations of the IUPHAR subcommittee on nomenclature of nAChR (Lukas et al., 1999).

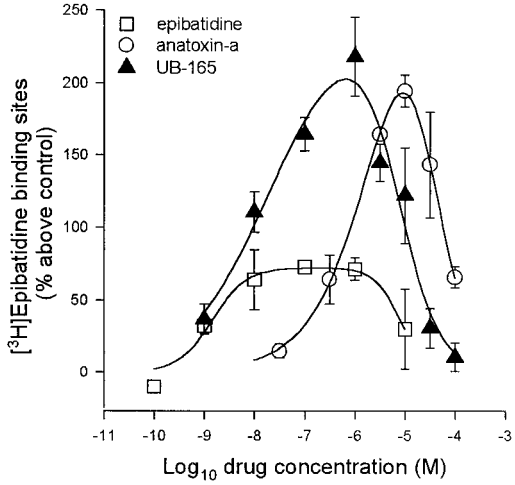

Figure 3. Upregulation of [^{3}H]-epibatidine binding sites expressed in M10 cells. M10 cells were cultured in the presence of dexamethasone and (±)-UB-165 (▲), (±)-anatoxin-a (○), or (±)-epibatidine (□) for 48 hr. After extensive washing, [^{3}H]-epibatidine binding was performed on M10 cells *in situ*. Upregulation was expressed as specific [^{3}H]-epibatidine binding above that of control cells treated in parallel with dexamethasone alone. (±)-Epibatidine was a partial agonist for upregulation compared with (±)-UB-165 and (±)-anatoxin-a. Each point is the result of at least three separate determinations ± SEM. Data points were fitted to a logistic equation (Whiteaker et al., 1998), giving EC_{50} values of 1.2 ± 0.2, 25.3 ± 17.7, and 985 ± 515 nM, and percentage maximum upregulation above control of 76.4 ± 5.7, 237 ± 47, and 221 ± 28%, for (±)-epibatidine, UB-165, and (±)-anatoxin-a, respectively.

[^{3}H]-dopamine release evoked by maximally effective concentrations of the four agonists mentioned above (Fig. 4*B*). The results confirm the differences in efficacy noted above. Although mecamylamine inhibited agonist-evoked [^{3}H]-dopamine release to the same extent in each case (the residual release being the nonspecific component that is elicited by a buffer pulse without agonist), α-conotoxin-MII produced varying degrees of inhibition. The mecamylamine-sensitive response to (±)-anatoxin-a was reduced by 56% by the toxin, in agreement with our previous findings (Kaiser et al., 1998), whereas the mecamylamine-sensitive [^{3}H]-dopamine release evoked by (±)-epibatidine and (−)-nicotine was inhibited by 47.9 and 32.4%, respectively. However, the mecamylamine-sensitive response to (±)-UB-165 was almost completely blocked (87.8%) by α-conotoxin-MII. This suggests that (±)-UB-165 has very little efficacy at the other subtype(s) of nAChRs responsible for [^{3}H]-dopamine release. Because the $\alpha4\beta2$ subtype is a candidate for this role, we examined the behavior of (±)-UB-165 in a neurochemical assay for this putative subtype.

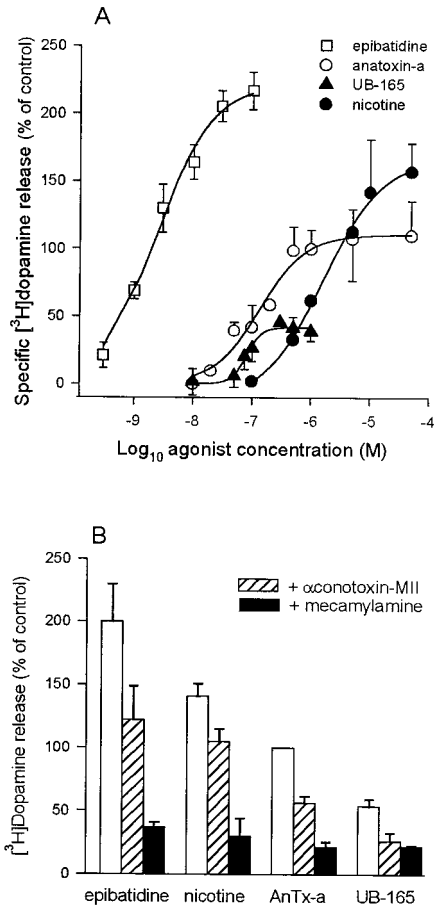

Figure 4. Nicotinic stimulation of [^{3}H]-dopamine release from rat striatal synaptosomes. *A*, Dose–response curves for the release of [^{3}H]-dopamine evoked by increasing concentrations of (±)-epibatidine (□), (−)-nicotine (●), (±)-anatoxin-a (○), and (±)-UB-165 (▲). Each agonist concentration was tested in the presence and absence of mecamylamine to determine specific nAChR-mediated release, as described in Materials and Methods. Responses were normalized to the response to 1 μM (±)-anatoxin-a, determined in parallel. Values are the mean ± SEM of at least three independent assays. The rank order of potencies (EC_{50} values) is (±)-epibatidine (2.4 ± 0.4 nM) > (±)-UB-165 (88 ± 18 nM) ≥ (±)-AnTx-a (134 ± 26 nM) > (−)-nicotine (1595 ± 377 nM). *B*, The inhibition by α-conotoxin-MII (112 nM; *hatched bars*) of [^{3}H]-dopamine release evoked by maximally effective concentrations of agonists is compared with inhibition by mecamylamine (10 μM; *black bars*). Synaptosomes loaded with [^{3}H]-dopamine were perfused with antagonist for 10 min before stimulation with (±)-epibatidine (0.1 μM), (−)-nicotine (10 μM), (±)-anatoxin-a (1 μM), or (±)-UB-165 (1 μM). Responses were normalized to the response to 1 μM (±)-anatoxin-a, determined in parallel. Values are the mean ± SEM of at least three independent assays.

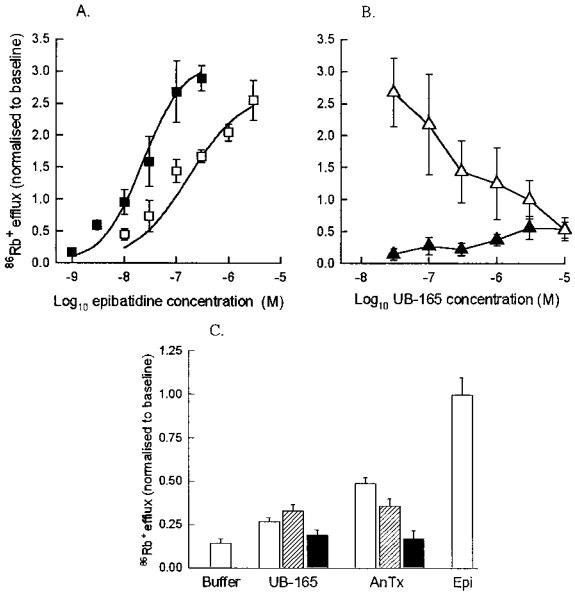

Figure 5. Nicotinic stimulation of $^{86}Rb^+$ efflux from thalamic synaptosomes. P2 synaptosomes from mouse (*A*, *B*) or rat (*C*) thalamus were loaded with $^{86}Rb^+$ and superfused; $^{86}Rb^+$ efflux is a measure of nAChR activation, primarily of the $\alpha4\beta2$ subtype (Marks et al., 1993). *A*, Dose–response curve of $^{86}Rb^+$ efflux stimulated by (±)-epibatidine, in the absence (■) or presence (□) of 1 μM (±)-UB-165. *B*, Dose–response curve of $^{86}Rb^+$ efflux stimulated by (±)-UB-165, in the absence (▲) or presence (△) of 100 nM (±)-epibatidine. *C*, Comparison of $^{86}Rb^+$ efflux from rat thalamic synaptosomes stimulated by maximally effective concentrations of (±)-UB-165 (1 μM), (±)-anatoxin-a (10 μM), and (±)-epibatidine (100 nM) (and buffer control). (±)-UB-165 and (±)-anatoxin-a were also tested in the presence of α-conotoxin-MII (112 nM; *hatched bars*) and mecamylamine (10 μM; *black bars*). Values are the mean ± SEM of at least three independent assays.

$^{86}Rb^+$ efflux from thalamic synaptosomes

The efflux of $^{86}Rb^+$ from preloaded mouse thalamic synaptosomes in response to nicotinic agonists is proposed to reflect the activation of $\alpha4\beta2$ nAChRs (Marks et al., 1993, 1996, 1999). (±)-UB-165 was compared with (±)-epibatidine for its ability to elicit $^{86}Rb^+$ efflux from this preparation (Fig. 5*A*,*B*). Although (±)-epibatidine was a potent and efficacious agonist in this assay (Fig. 5*A*), as reported previously (Marks et al., 1996), (±)-UB-165 produced very little response when tested over the concentration range examined in the [^{3}H]-dopamine release assay (Fig. 5*B*). Indeed, 1 μM (±)-UB-165 elicited <15% of the maximum $^{86}Rb^+$ efflux provoked by (±)-epibatidine. The interpretation that (±)-UB-165 is a partial agonist with respect to $^{86}Rb^+$ efflux is supported by the ability of (±)-UB-165 (1 μM) to shift the dose–response curve for (±)-epibatidine to the right (Fig. 5*A*). Moreover, increasing concentrations of (±)-UB-165 progressively inhibited the response to a maximally effective concentration of (±)-epibatidine (100 nM) (Fig. 5*B*). The low efficacy of (±)-UB-165 in eliciting $^{86}Rb^+$ efflux was verified in rat thalamic synaptosomes (Fig. 5*C*). Maximally effective concentrations of (±)-UB-165, (±)-anatoxin-a, and (±)-epibatidine with respect to [^{3}H]-dopamine release were compared. Their relative efficacies in stimulating $^{86}Rb^+$ efflux resemble their efficacies in evoking α-conotoxin-MII-insensitive [^{3}H]-dopamine release (Fig. 4*B*). Indeed, the slight increase in $^{86}Rb^+$ efflux in response to (±)-UB-165 was blocked by mecamylamine but was insensitive to α-conotoxin-MII (Fig. 5*C*).

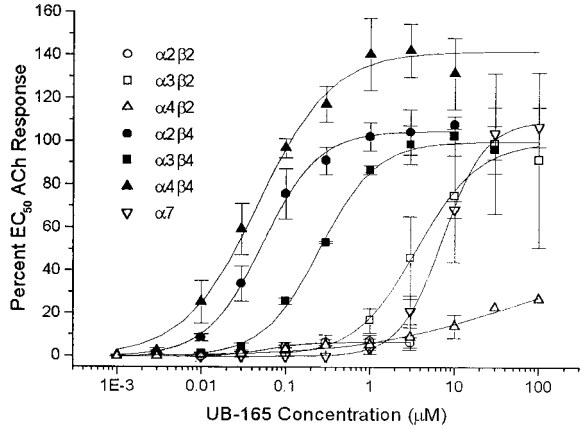

Figure 6. Concentration–response curves for (±)-UB-165 at recombinant human nAChRs. Pairwise combinations of human α and β subunits, or α7 alone, were expressed in *Xenopus* oocytes. Current responses in each oocyte were normalized to an EC_{50} concentration of ACh. EC_{50} values yielded by logistical curve fits were 3.9 μM for $\alpha3\beta2$ (□), 0.05 μM for $\alpha2\beta4$ (●), 0.27 μM for $\alpha3\beta4$ (■), 0.05 μM for $\alpha4\beta4$ (▲), and 6.9 μM for α7 (▽). There was little activation of $\alpha2\beta2$ (○) and $\alpha4\beta2$ (△) subtypes. Data points represent mean ± SD of three to six experiments.

Activation of inward currents in *Xenopus* oocytes expressing nAChRs of defined subunit combination

To confirm that UB-165 has low efficacy at $\alpha4\beta2$ nAChRs, and to assess its efficacy at other nAChR subtypes, it was examined for its ability to elicit inward currents in *Xenopus* oocytes expressing pairwise combinations of human α and β subunits, or homo-oligomeric nAChRs of α7 subunits (Fig. 6). (±)-UB-165 was most potent in activating $\alpha4\beta4$ and $\alpha2\beta4$ nAChRs (EC_{50} = 0.05 μM), followed by $\alpha3\beta4$ (0.27 μM), $\alpha3\beta2$ (3.9 μM), and α7 (6.9 μM), and was similarly efficacious at these subtypes. In contrast, (±)-UB-165 failed to elicit significant currents from oocytes expressing $\alpha4\beta2$ or $\alpha2\beta2$ nAChRs.

Activation of Ca^{2+} fluxes in the SH-SY5Y cell line

The functional potency of (±)-UB-165 at native α3-containing nAChRs was investigated in the human neuroblastoma cell line SH-SY5Y. Because this cell line does not express α4 subunits, it was used to examine the efficacy of UB-165 at native nAChRs other than the $\alpha4\beta2^*$ subtype. Receptor activation was assayed as an increase in intracellular Ca^{2+}, measured quantitatively in suspensions of SH-SY5Y cells using fura-2 (Fig. 7). (±)-UB-165 and (±)-anatoxin-a were compared: both agonists increased intracellular Ca^{2+}, and this effect was totally blocked by 10 μM mecamylamine (Fig. 7*A*,*B*). Determination of dose–response relationships showed that (±)-UB-165 was more potent than (±)-anatoxin-a, with EC_{50} values of 154 ± 20 and 530 ± 92 nM, respectively (Fig. 7*C*). Comparison of maximally effective concentrations of each drug (1 μM (±)-UB-165 and 10 μM (±)-anatoxin-a) showed them to be comparably efficacious in this assay (Fig. 7*D*). Increases in intracellular Ca^{2+} evoked by these maximally stimulating drug concentrations were partially blocked to the same extent by 112 nM α-conotoxin-MII (43.9 ± 8.3 and 49.8 ± 10.0% inhibition of (±)-UB-165- and (±)-anatoxin-a-evoked Ca^{2+} responses, respectively) (Fig. 7*D*).

DISCUSSION

The potent nicotinic agonists epibatidine and anatoxin-a are structurally related in that they both incorporate an azobicyclic core (Fig. 1); UB-165 is a hybrid molecule comprising the bulkier

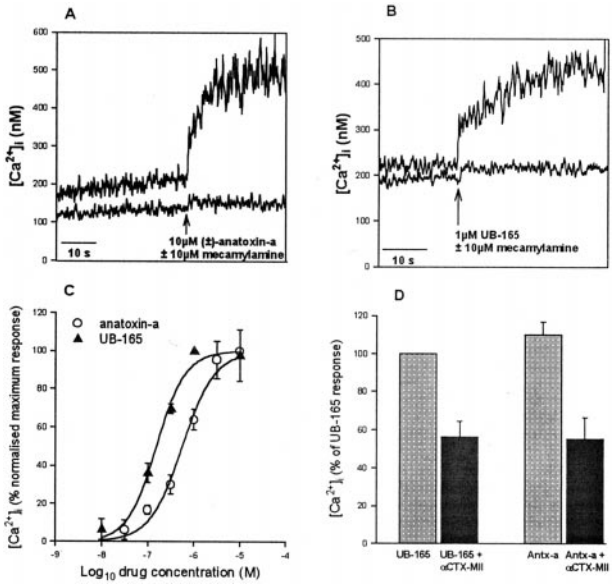

Figure 7. Nicotinic stimulation of increases in intracellular Ca^{2+} in SH-SY5Y cells. SH-SY5Y cells were loaded with 5 μM fura-2 AM in Ca^{2+}-free buffer for 45 min before addition of 2 mM $CaCl_2$ followed by (±)-anatoxin-a or (±)-UB-165. Antagonists were added 5 min before the addition of Ca^{2+} and agonist. Representative fluorimetry traces in response to 10 μM (±)-anatoxin-a (*A*) and 1 μM (±)-UB-165 (*B*). The *bottom trace* in *A* and *B* shows the response in the presence of 10 μM mecamylamine. *C*, Dose–response relationships of increases in intracellular Ca^{2+} induced by (±)-anatoxin-a (○) and (±)-UB-165 (▲). For each curve, results were normalized to the responses produced by a maximally effective concentration of agonist, determined in parallel in the same experiment. Data points are the mean ± SEM of three independent assays and were fitted to the Hill equation, giving EC_{50} values of 154 and 530 nM for (±)-UB-165 and (±)-anatoxin-a, respectively. *D*, Comparison of efficacies of maximally stimulating concentrations of (±)-UB-165 (1 μM) and (±)-anatoxin-a (10 μM), and inhibition by α-conotoxin-MII (112 nM, *black bars*). Values are the mean of three independent experiments ± SEM and were normalized to the response to (±)-UB-165 within each separate experiment.

azobicyclo[4.2.1]nonane moiety of anatoxin-a attached to the chloropyridyl substituent of epibatidine (Wright et al., 1997). At $\alpha4\beta2$* and $\alpha3$-containing nAChR binding sites (defined by [^{3}H]-nicotine binding to brain membranes and [^{3}H]-epibatidine binding to SH-SY5Y cell membranes, respectively), UB-165 has intermediate potency, compared with the parent compounds (Fig. 2). It resembles epibatidine in its high degree of discrimination between $\alpha4\beta2$* binding sites on the one hand versus $\alpha7$ and muscle sites on the other (Table 1). In contrast, UB-165 is more like anatoxin-a with regard to its enantiospecificity (Wright et al., 1997) and its efficacy in upregulating $\alpha4\beta2$ nAChRs in M10 cells (Fig. 3). From these properties and its structural features it was not possible to predict the very low efficacy of UB-165 with regard to striatal [^{3}H]-dopamine release, measured in perfused synaptosome preparations *in vitro.* Use of the $\alpha3\beta2$-selective α-conotoxin-MII (Cartier et al., 1996) has enabled us to show that this low efficacy of UB-165 arises from its almost complete inability to activate the α-conotoxin-MII-insensitive component of nAChR-stimulated [^{3}H]-dopamine release. The failure of UB-165 to activate $\alpha4\beta2$*-mediated $^{86}Rb^+$ efflux from thalamic synaptosomes and to elicit responses in oocytes expressing $\alpha4\beta2$ nAChRs provides support for the proposition that presynaptic $\alpha4\beta2$* nAChRs on striatal dopaminergic terminals contribute to the nicotinic stimulation of [^{3}H]-dopamine release, in addition to $\alpha3\beta2$-containing nAChRs (Kulak et al., 1997; Kaiser et al., 1998).

Neurons in the substantia nigra pars compacta of the rat express mRNA for $\alpha3$, $\alpha4$, $\alpha5$, $\alpha6$, $\beta2$, and $\beta3$ (Wonnacott, 1997) and possibly $\beta4$ and $\alpha7$ subunits (Charpantier et al., 1998), and some or all of these may contribute to nAChRs on dopaminergic terminals in the striatum. The challenge of defining the subunit composition of native nAChRs responsible for particular physiological responses is important for understanding the significance of subunit heterogeneity, rules of assembly, and functional implications arising from receptor subtypes with differing properties. Nicotine-evoked [^{3}H]-dopamine release from striatal synaptosomes is absent from $\beta2$ null mutant mice (Grady et al., 1998), implicating the $\beta2$ subunit in all nAChRs in dopaminergic terminals governing this response in the mouse. Sensitivity to α-conotoxin-MII (Kulak et al., 1997; Kaiser et al., 1998), a toxin with specificity for the $\alpha3\beta2$ subunit combination expressed in *Xenopus* oocytes (Cartier et al., 1996; Kaiser et al., 1998) is compatible with the requirement for $\beta2$ to be present. This does not exclude the presence of additional types of subunit in an nAChR containing $\alpha3$ and $\beta2$ subunits. The restricted distributions of $\alpha6$ and $\beta3$ mRNA in the CNS, with high expression in the substantia nigra pars compacta (Deneris et al., 1989; Le Novère et al., 1996; Charpantier et al., 1998), together with the erstwhile "orphan" status of the $\alpha6$ and $\beta3$ subunits, makes them prime candidates for complex combinations with other subunits such as $\alpha3$ and $\beta2$ (Fucile et al., 1998; Groot-Kormelink et al., 1998).

A striking observation from the studies with α-conotoxin-MII is its incomplete inhibition of nicotinic agonist-evoked [^{3}H]-dopamine release. Kulak et al. (1997) found a block of 34–49% of (−)-nicotine-stimulated [^{3}H]-dopamine release, whereas Kaiser et al. (1998) reported 56% inhibition of mecamylamine-sensitive release evoked by (±)-anatoxin-a. The present study reproduces these findings and extends the analysis to other agonists. A partial inhibition (48%) of [^{3}H]-dopamine release evoked by (±)-epibatidine was observed, whereas the response evoked by (±)-UB-165 was almost totally inhibited by α-conotoxin-MII (Fig. 4). This suggests that (±)-UB-165 primarily activates only the α-conotoxin-MII-sensitive nAChRs associated with dopaminergic terminals, which accords with an $\alpha3\beta2$-containing nAChR. The magnitude of the α-conotoxin-MII-sensitive portion of evoked [^{3}H]-dopamine release is rather similar between agonists (with the exception of (±)-epibatidine, for which considerable variability was encountered), whereas the α-conotoxin-MII-insensitive portion varies in the ratio 1:0.88:0.40:0.04 for (±)-epibatidine, (−)-nicotine, (±)-anatoxin-a, and (±)-UB-165, respectively. This variation in the α-conotoxin-MII-insensitive responses to different agonists is largely responsible for their different efficacies with respect to total release (Fig. 4*B*).

The hypothesis, elaborated in the introductory remarks, states that the α-conotoxin-MII-insensitive component of nAChR-evoked striatal dopamine release is mediated by $\alpha4\beta2$* nAChRs. The low efficacy, and complete block by α-conotoxin-MII, of UB-165-evoked [^{3}H]dopamine release (Fig. 4) leads to the prediction that (±)-UB-165 should be a very poor agonist at this receptor subtype. nAChR-evoked $^{86}Rb^+$ efflux from mouse thalamic synaptosomes is attributed to an $\alpha4\beta2$* nAChR (Marks et al., 1993, 1996), and, in agreement with this prediction, UB-165 is a very weak, partial agonist in this assay (Fig. 5). In rat thalamic synaptosomes, (±)-epibatidine, (±)-anatoxin-a, and (±)-UB-165 stimulated mecamylamine-sensitive $^{86}Rb^+$ efflux with relative efficacies of 1:0.39:0.08, very comparable to the ratio of efficacies

for α-conotoxin-MII-insensitive [^{3}H]-dopamine release (see above). Moreover, Type II responses in rat hippocampal neurons, attributed to an α4β2 nAChR, show different efficacies with different agonists, with the ratio 1:0.6:0.3 for (+)-epibatidine, (−)-nicotine, and (+)-anatoxin-a, respectively (Alkondon and Albuquerque, 1995), similar to those found here for these agonists, with respect to α-conotoxin-MII-insensitive [^{3}H]-dopamine release and $^{86}Rb^+$ efflux.

Results from *Xenopus* oocytes expressing various recombinant nAChR subtypes verify that (±)-UB-165 has low efficacy at α4β2 nAChRs. The only other subunit combination examined at which (±)-UB-165 was inefficacious was α2β2 (Fig. 6), but the lack of expression of α2 in substantia nigra (Wada et al., 1989) excludes this as a contributor to the presynaptic modulation of striatal dopamine release. The electrophysiological analysis confirms that UB-165 is a full agonist at α3β2 nAChRs. This is consistent with the data from a functional assay for native α3-containing nAChRs [increases in intracellular Ca^{2+} in SH-SY5Y cells (Fig. 7)], in which (±)-anatoxin-a and (±)-UB-165 were equally efficacious and equally sensitive to α-conotoxin-MII. SH-SY5Y cells expresses mRNA for α3, α5, α7, β2, and β4 nAChR subunits (Lukas et al., 1993; Peng et al., 1994). Therefore the α4β2 nAChR is not present in this cell line. Nevertheless, inhibition by α-conotoxin-MII was incomplete (~50%) (Fig. 7), and this presumably reflects the presence of additional nAChR subtypes that lack an α3β2 interface, in particular β4-containing nAChRs. Heterogeneous combinations of α3, α5, β2, and β4 subunits in SH-SY5Y cells have been proposed, on the basis of immunoisolation of nAChRs using subunit-specific antibodies (Wang et al., 1996). Notably, 56% of α3-containing nAChRs were found to contain the β2 subunit. The α-conotoxin-MII-insensitive response is likely to arise from activation of α3β4-containing nAChRs that lack the β2 subunit (although a contribution from α7-type nAChRs cannot be ruled out). α3β4 nAChRs expressed in *Xenopus* oocytes are insensitive to the concentration of α-conotoxin-MII used in this study (Cartier et al., 1996; Kaiser et al., 1998) but are fully activated by UB-165 (Fig. 6). Moreover, the comparable efficacies of (±)-UB-165- and (±)-anatoxin-a demonstrate that the α-conotoxin-MII-insensitive component of nAChR-mediated Ca^{2+} increases in SH-SY5Y cells is clearly different from the α-conotoxin-MII-insensitive component of nAChR-mediated [^{3}H]-dopamine release from striatal synaptosomes.

The weak partial agonism of UB-165 at α4β2* nAChRs contrasts with its full efficacy in upregulating α4β2 nAChRs in M10 cells (Fig. 3). Lower concentrations of agonist are needed to induce upregulation, compared with those required to elicit functional responses. Together with the general inability of antagonists to prevent agonist-induced upregulation, a higher affinity state of the nAChRs than the active conformation is implicated as the trigger for the upregulation of binding sites (Whiteaker et al., 1998; Fenster et al., 1999). Whether this state is the high-affinity desensitized state measured in ligand binding assays remains controversial. This result demonstrates that although UB-165 lacks functional efficacy at α4β2* nAChRs, long-term exposure to this drug would upregulate this receptor subtype with potential functional consequences.

UB-165 is not unique as a partial agonist in stimulating [^{3}H]-dopamine release (Holladay et al., 1997) and $^{86}Rb^+$ efflux (Marks et al., 1996). For example RJR 2429 has a structure comparable to UB-165, comprising an azobicyclo[2.2.2]octane core coupled to a chloropyridyl moiety (Bencherif et al., 1998), and has a profile similar to UB-165 in functional and binding assays, except for its much higher potency at muscle nAChRs. However, application of novel ligands in conjunction with selective antagonists is necessary to maximize their potential as tools to discriminate receptor subtypes. This study has exploited the exquisite subtype selectivity of α-conotoxin-MII together with the partial agonism of UB-165 to arrive at a better definition of the nAChR subtypes present on dopamine terminals in striatal preparations. The conclusion that both α4β2*- and α3β2-containing nAChRs contribute to [^{3}H]-dopamine release, either on the same or separate populations of terminals (varicosities), enhances our understanding of this model system and raises further questions about the physiological purpose of nAChRs in the mammalian brain.

REFERENCES

Alkondon M, Albuquerque EX (1995) Diversity of nicotinic acetylcholine receptors in rat hippocampal neurons. III. Agonist actions of the novel alkaloid epibatidine and analysis of type II current. J Pharmacol Exp Ther 274:771–782.

Alkondon M, Pereira EF, Albuquerque EX (1998) Alpha-bungarotoxin- and methyllycaconitine-sensitive nicotinic receptors mediate fast synaptic transmission in interneurons of rat hippocampal slices. Brain Res 810:257–263.

Bencherif M, Schmitt JD, Bhatti BS, Crooks P, Caldwell WS, Lovette ME, Fowler K, Reeves L, Lippiello PM (1998) The heterocyclic substituted pyridine derivative (±)-2-(-3-pyridinyl)-1-azabicyclo [2.2.2]octane (RJR-2429): a selective ligand at nicotinic acetylcholine receptors. J Pharmacol Exp Ther 284:886–894.

Cartier GE, Yoshokami D, Gray WR, Luo S, Olivera BM, McIntosh JM (1996) A new α-conotoxin which targets α3β2 nicotinic acetylcholine receptors. J Biol Chem 271:7522–7528.

Charpantier E, Barneoud P, Moser P, Besnard F, Sgard F (1998) Nicotinic acetylcholine subunit mRNA expression in dopaminergic neurons of the rat substantia nigra and ventral tegmental area. NeuroReport 9:3097–3101.

Chavez-Noriega LE, Crona JH, Washburn MS, Urrutia A, Elliott KJ, Johnson EC (1997) Pharmacological characterization of recombinant human neuronal nicotinic acetylcholine receptors hα2β2, hα2β4, hα3β2, hα3β4, hα4β2, hα4β4 and hα7 expressed in *Xenopus* oocytes. J Pharmacol Exp Ther 280:346–356.

Cheng Y-C, Prusoff WH (1973) Relationship between the inhibition constant (K_i) and the concentration of the inhibitor which causes 50 percent inhibition (IC_{50}) of an enzymatic reaction. Biochem Pharmacol 22:3089–3108.

Clarke PBS, Pert A (1985) Autoradiographic evidence for nicotine receptors on nigrostriatal and mesolimbic dopaminergic neurons. Brain Res 348:355–358.

Dani JA, Heinemann S (1996) Molecular and cellular aspects of nicotine abuse. Neuron 16:905–908.

Davies ARL, Hardick DJ, Blagbrough IS, Potter BVL, Wolstenholme AJ, Wonnacott S (1999) Characterisation of the binding of [^{3}H]methyllycaconitine: a new radioligand for labelling α7-type neuronal nicotinic acetylcholine receptors. Neuropharmacology 38:679–690.

Decker MW, Arneric SP (1998) Nicotinic acetylcholine receptor-targeted compounds: a summary of the developmental pipeline and therapeutic potential. In: Neuronal nicotinic receptors, pharmacology and therapeutic opportunities (Arneric SP, Brioni JD, eds), pp 395–411. New York: Wiley.

Deneris ES, Boulter J, Swanson LW, Patrick J, Heinemann S (1989) Beta3: A new member of nicotinic acetylcholine receptor gene family is expressed in brain. J Biol Chem 264:6268–6272.

Elliott KJ, Ellis SB, Berckhan KJ, Urrutia A, Chavez-Noriega LE, Johnson EC, Velicelebi G, Harpold MM (1996) Comparative structure of human neuronal alpha 2-alpha 7 and beta 2-beta 4 nicotinic acetylcholine receptor subunits and functional expression of the alpha 2, alpha 3, alpha 4, alpha 7, beta 2, and beta 4 subunits. J Mol Neurosci 7:217–228.

El-Bizri H, Clarke PBS (1994) Blockade of nicotinic receptor-mediated release of dopamine from striatal synaptosomes by chlorisondamine and other nicotinic antagonists administered in vitro. Br J Pharmacol 111:406–413.

Fenster CP, Whitworth TL, Sheffield EB, Quick MW, Lester RAJ (1999) Up-regulation of surface $\alpha4\beta2$ nicotinic receptors is initiated by receptor desensitization after chronic exposure to nicotine. J Neurosci 19: 4804–4814.

Frazier CJ, Buhler AV, Weiner JL, Dunwiddle TV (1998) Synaptic potentials mediated via α-bungarotoxin-sensitive nicotinic acetylcholine receptors in rat hippocampal interneurons. J Neurosci 18:8228–8235.

Fucile S, Matter J-M, Erkman L, Ragozzino D, Barabino B, Grassi F, Alemà S, Ballivet M, Eusebi F (1998) The neuronal alpha6 subunit forms heteromeric acetylcholine receptors in human transfected cells. Eur J Neurosci 10:172–178.

Garcha HS, Thomas P, Spivak CE, Wonnacott S, Stolerman IP (1993) Behavioural and ligand-binding studies in rats with 1-acetyl-4-methylpiperazine, a novel nicotinic agonist. Psychopharmacology 110:347–354.

Grady S, Marks MJ, Wonnacott S, Collins AC (1992) Characterization of nicotinic receptor-mediated [^{3}H]dopamine release from synaptosomes prepared from mouse striatum. J Neurochem 59:848–856.

Grady S, Grun EU, Marks MJ, Collins AC (1997) Pharmacological comparison of transient and persistent [^{3}H]dopamine release from mouse striatal synaptosomes and response to chronic L-nicotine treatment. J Pharmacol Exp Ther 282:32–43.

Grady SR, Lu Y, Picciotto MR, Changeux J-P, Collins AC (1998) Nicotine-stimulated synaptosomal neurotransmitter release from $\beta2$ null mutant mice. Soc Neurosci Abstr 28:530.15.

Groot-Kormelink PJ, Luyten WH, Colquhoun D, Sivilotti LG (1998) A reporter mutation approach shows incorporation of the "orphan" subunit beta3 into a functional nicotinic receptor. J Biol Chem 273:15317–15320.

Grynkiewicz G, Poenie, Tsien RY (1985) A new generation of Ca^{2+} indicators with greatly improved fluorescence properties. J Biol Chem 260:3440–3450.

Holladay MW, Dart MJ, Lynch JK (1997) Neuronal nicotinic acetylcholine receptors as targets for drug discovery. J Med Chem 40:4169–4194.

Kaiser SA, Soliakov L, Harvey SC, Leutje CW, Wonnacott S (1998) Differential inhibition by α-conotoxin-MII of the nicotinic stimulation of [^{3}H]dopamine release from rat striatal synaptosomes and slices. J Neurochem 70:1069–1076.

Kulak JM, Nguyen TA, Olivera BM, McIntosh JM (1997) α-Conotoxin MII blocks nicotine-stimulated dopamine release in rat striatal synaptosomes. J Neurosci 17:5263–5270.

Le Novère N, Zoli M, Changeux J-P (1996) Neuronal nicotine receptor $\alpha6$ subunit mRNA is selectively concentrated in catecholaminergic nuclei of the rat brain. Eur J Neurosci 8:2428–2439.

Lukas RJ, Norman SA, Lucero L (1993) Characterization of nicotinic acetylcholine receptors expressed by cells of the SH-SY5Y human neuroblastoma clonal line. Mol Cell Neurosci 4:1–12.

Lukas RJ, Changeux J-P, le Novère N, Albuquerque EX, Balfour DJK, Berg DK, Bertrand D, Chiappinelli VA, Clarke PBS, Collins AC, Dani JA, Grady SA, Kellar KJ, Lindstrom JM, Marks MJ, Quik M, Taylor PW, Wonnacott S (1999) International Union of Pharmacology. XX. Current status of the nomenclature for nicotinic acetylcholine receptors and their subunits. Pharmacol Rev 51:397–401.

Marks MJ, Farnham DA, Grady SR, Collins AC (1993) Nicotinic receptor function determined by stimulation of rubidium efflux from mouse brain synaptosomes. J Pharmacol Exp Ther 264:542–552.

Marks MJ, Robinson SF, Collins AC (1996) Nicotinic agonists differ in activation and desensitization of $^{86}Rb^+$ efflux from mouse thalamic synaptosomes. J Pharmacol Exp Ther 277:1383–1396.

Marks MJ, Whiteaker P, Calcaterra J, Stitzel JA, Bullock AE, Grady SR, Picciotto MR, Changeux J-P, Collins AC (1999) Two pharmacologically distinct components of nicotinic receptor-mediated rubidium efflux in mouse brain require the $\beta2$ subunit. J Pharmacol Exp Ther 289:1090–1103.

McIntosh JM, Santos AD, Olivera BM (1999) Conus peptides targeted to specific nicotinic acetylcholine receptor subtypes. Annu Rev Biochem 68:59–88.

Murphy NP, Vaughan PFT, Ball SG, McCormack JG (1991) The cholinergic regulation of intracellular calcium in the human neuroblastoma, SH-SY5Y. J Neurochem 57:2116–2123.

Peng X, Katz M, Gerzanich V, Anand R, Lindstrom J (1994) Human $\alpha7$ acetylcholine receptor: cloning of the $\alpha7$ subunit from the SH-SY5Y cell line and determination of pharmacological properties of native receptors and functional $\alpha7$ homomers expressed in *Xenopus* oocytes. Mol Pharmacol 45:546–554.

Rapier C, Lunt GG, Wonnacott S (1990) Nicotinic modulation of [^{3}H]dopamine release from striatal synaptosomes: pharmacological characterisation. J Neurochem 54:937–945.

Role LW, Berg DK (1996) Nicotinic receptors in the development and modulation of CNS synapses. Neuron 16:1077–1085.

Romm E, Lippiello PM, Marks MJ, Collins AC (1990) Purification of [l-[^{3}H]nicotine eliminates low affinity binding. Life Sci 46:935–945.

Sacaan AI, Dunlop JL, Lloyd GK (1995) Pharmacological characterisation of neuronal acetylcholine gated ion channel receptor-mediated hippocampal norepinephrine and striatal dopamine release from rat brain slices. J Pharmacol Exp Ther 274:224–230.

Soliakov L, Wonnacott S (1996) Voltage-sensitive Ca^{2+} channels involved in nicotinic receptor-mediated [^{3}H]dopamine release from rat striatal synaptosomes. J Neurochem 67:163–170.

Soliakov L, Gallagher T, Wonnacott S (1995) Anatoxin-a evoked [^{3}H]-dopamine release from rat striatal synaptosomes. Neuropharmacology 34:1535–1541.

Wada E, Wada K, Boulter J, Deneris E, Heinemann S, Patrick J, Swanson L (1989) Distribution of alpha2, alpha3, alpha4, and beta 2 neuronal nicotinic receptor subunit mRNAs in the central nervous system: a hybridization histochemical study in the rat. J Comp Neurol 284:314–335.

Wang F, Gerzanich V, Wells G, Anand R, Peng X, Keyser K, Lindstrom J (1996) Assembly of human neuronal nicotinic receptor $\alpha5$ subunits with $\alpha3$, $\beta2$ and $\beta4$ subunits. J Biol Chem 271:17656–17685.

Whiteaker P, Sharples CGV, Wonnacott S (1998) Agonist induced up-regulation of $\alpha4\beta2$ nicotinic acetylcholine receptors in M10 cells: pharmacological and spatial definition. Mol Pharmacol 53:950–962.

Wonnacott S (1997) Presynaptic nicotinic ACh receptors. Trends Pharmacol Sci 20:92–98.

Wright E, Gallagher T, Sharples CGV, Wonnacott S (1997) Synthesis of UB-165: a novel nicotinic ligand and anatoxin-a/epibatidine hybrid. Bioorg Med Chem Lett 7:2867–2870.

Zoli M, Léna C, Picciotto MR, Changeux J-P (1998) Identification of four classes of brain nicotinic receptors using $\beta2$ mutant mice. J Neurosci 18:4461–4472.